Synthesis and Properties of New Thermoplastic Polymers from Substituted 3,4-Dihydro-2*H*-1,3-benzoxazines

Yong-Xia Wang and Hatsuo Ishida*

The NSF Center for Molecular and Microstructure of Composites (CMMC), Department of Macromolecular Science, Case Western Reserve University, Cleveland, Ohio 44106-7202

Received June 8, 1999; Revised Manuscript Received January 17, 2000

ABSTRACT: With phosphorus pentachloride (PCl_5) as a cationic initiator, new benzoxazine-based semicrystalline and amorphous thermoplastics with significant molecular weights have been synthesized for the first time. ^1H and ^{13}C nuclear magnetic resonance spectroscopy, Fourier transform infrared spectroscopy, and elemental analysis are used to characterize the resulting polymers. Both Mannich base phenoxy-type (Type I) and Mannich base phenolic-type (Type II) polybenzoxazines are obtained. The polymer properties have been studied by differential scanning calorimetry, thermogravimetric analysis, and wide-angle X-ray diffraction.

Introduction

Benzoxazines are bicyclic heterocycles generated by the Mannich-like condensation of a phenol, formaldehyde, and an amine.[1−6] They have long been recognized for their wide range of biological activity with uses as herbicides and agricultural microbiocides, as well as bactericides, fungicides, and antitumor agents.[7−9] On the other hand, polybenzoxazines, one of a series of phenolic-type polymers, which are generated upon thermal polymerization from various types of substituted 3,4-dihydro-2*H*-1,3-benzoxazines, offer excellent mechanical, physical, and thermal properties due to the phenolic groups, Mannich base linkages, and the existence of extensive inter- and intramolecular hydrogen bonds.[10−12]

Work concerning the catalyst assisted polymerization of benzoxazines has been reported. Burke et al.[13] discovered that benzoxazine rings react preferentially with the ortho positions of free phenolic compounds to form a dimer with a Mannich base bridge structure. Also, Riess et al.[14] characterized the high reactivity of the ortho position by following the kinetics of monofunctional benzoxazines with 2,4-di-*tert*-butylphenol as a catalyst. More recently, Ishida et al.[15−17] investigated a series of acids, alkalies, and a Lewis acid, $BF_3O(Et)_2$, as curing agents for bisphenol A-based benzoxazines. They found that some of the catalysts tested, for example, adipic acid, can effectively decrease the induction time for the benzoxazine curing and increase the reaction rate. Gu and co-workers[18,19] also confirmed that some organic acids and Lewis acids could catalyze the ring-opening polymerization of benzoxazines. Nevertheless, the molecular weight of all the reported polybenzoxazines derived from mono-oxazine ring containing benzoxazine monomers are usually too low (several hundred to a few thousand) to have structural applications.

Compared to the well-developed studies of the thermal polymerization of benzoxazines with or without initiators or catalysts in the absence of solvent, only a few studies of the solution polymerization of 3,4-dihydro-2*H*-1,3-benzoxazines, with the help of initiators, have been reported.[20] Unlike bulk thermal polymerization, solvent-borne ionic polymerization allows better control of the molecular weight and molecular structure of the resulting polymer, thereby simplifying characterization. In our previous work, various cationic, anionic, and radical polymerization initiators have been tested to initiate the benzoxazine ring-opening polymerization.[20] The results show that the ring-opening polymerization of the benzoxazine family follows a cationic mechanism. Among the tested initiators, phosphorus pentachloride (PCl_5) has been chosen for this study. In this paper, we will report the cationic ring-opening polymerization of a series of mono-oxazine ring containing substituted 3,4-dihydro-2*H*-1,3 benzoxazines.

Experimental Section

Materials. All reagents were purchased from Aldrich. The formaldehyde was 37 wt % in water. The phenolic compounds used for the synthesis of monomers are *p*-cresol, 2,4-dimethyl phenol, 2,3,5-trimethyl phenol, and 3,4,5-trimethyl phenol with purities of 99%, 95%, 97%, and 99%, respectively. Phosphorus pentachloride, 95%, was used without further purification. Chloroform (polymerization solvent) was purified by the following method: washed with water, dried over sodium sulfate, refluxed and distilled over phosphorus pentoxide under N_2 protection, and stored in an argon atmosphere drybox (1 ppm moisture rated) before use.

Monomer Synthesis. The four benzoxazine monomers as shown in Scheme 1, 3-methyl-3,4-dihydro-6-methyl-2*H*-1,3-benzoxazine (I), designated as *p*C-m, 3-methyl-3,4-dihydro-6,8-dimethyl-2*H*-1,3-benzoxazine (II), designated as 24DMP-m, 3-methyl-3,4-dihydro-5,7,8-trimethyl-2*H*-1,3-benzoxazine (III), designated as 235TMP-m, and 3-methyl-3,4-dihydro-5,6,7-trimethyl-2*H*-1,3-benzoxazine (IV), designated as 345TMP-m, were synthesized following the procedure described by Dunkers and Ishida[21] with a few essential modifications. The mole ratio of the reagents, amine:formaldehyde:phenol, was 1:2:1. Other than the method described in the reference, all the monomers were further purified by recrystallization from hexane or hexane/methylene chloride three times, dried under vacuum over Drierite for 3 days. *p*C-m was also further purified by sublimation. The purity of the monomers was verified by gas chromatography/mass spectroscopy (GC/MS) analysis. The results of the monomer synthesis are summarized as follows.

pC-m. White needlelike crystals. Purity: 99.97%. ^1H NMR (200 MHz, $CDCl_3$, 298 K): δ 2.25 (Ar−CH_3), 2.59 (N−CH_3), 3.91(Ar−CH_2−N), 4.76 (O−CH_2−N), and 6.67−6.94 (3H, Ar−H). ^{13}C NMR (200 MHz, DMSO, 298K): δ 20.08 (Ar−C), 39.08 (N−C), 51.29 (Ar−C−N), 83.14 (O−C−N), 115.47 (Ar), 119.70 (Ar), 127.76 (2C, Ar), 128.71 (Ar), and 151.18 (Ar).

10.1021/ma9909096 CCC: $19.00
Published on Web 03/23/2000

Scheme 1. Monomer Synthesis

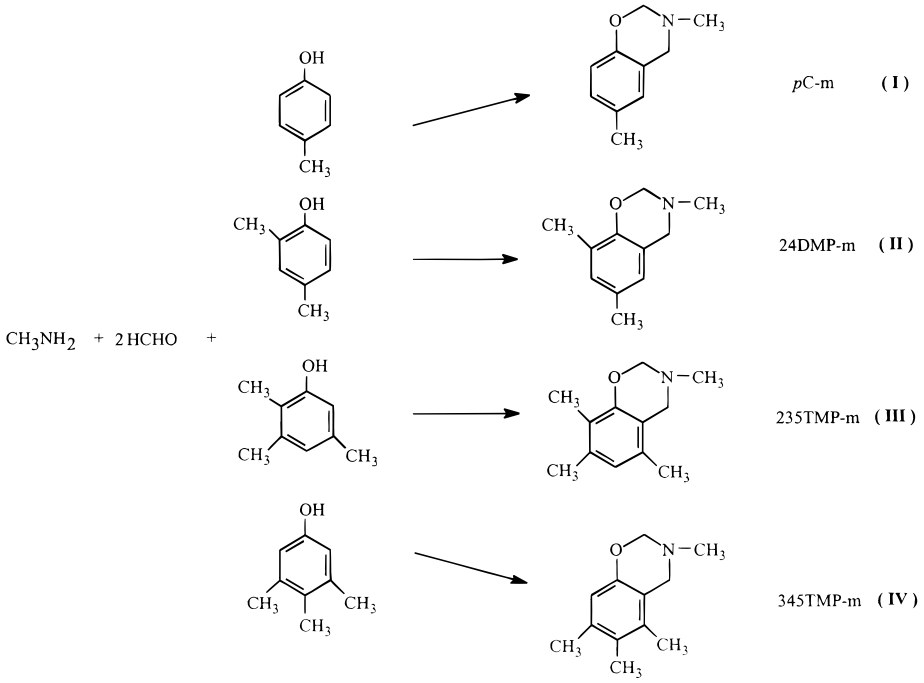

24DMP-m. Colorless liquid/spherulites. Purity: 99.93%. ^{1}H NMR (200 MHz, $CDCl_3$, 298K): δ 2.15, 2.21 (2 Ar−CH_3), 2.58 (N−CH_3), 3.90 (Ar−CH_2−N), 4.77 (O−CH_2−N), 6.61,6.80 (2H, Ar−H). ^{13}C NMR (200 MHz, DMSO, 298K): δ 15.11 (Ar−C), 20.05 (Ar−C), 39.14 (N−C), 51.76 (Ar−C−N), 83.42 (O−C−N), 119.08 (Ar), 123.99 (Ar), 125.25 (Ar), 127.99 (Ar), 129.10 (Ar), 149.38 (Ar).

235TMP-m. White flakelike crystals. Purity: 99.95%. ^{1}H NMR (200 MHz, $CDCl_3$, 298K): δ 2.06, 2.11, 2.24 (Ar−CH_3), 2.59 (N−CH_3), 3.82 (Ar−CH_2−N), 4.74 (N−CH_2−O), 6.54 (Ar−H). ^{13}C NMR (200 MHz, $CDCl_3$, 298K): δ 10.92 (Ar−C), 17.58 (Ar−C), 19.44 (Ar−C), 38.67 (N−C), 49.96 (Ar−C−N), 82.80 (O−C−N), 115.62 (Ar), 120.02 (Ar), 122.79 (Ar), 132.18 (Ar), 134.26 (Ar), 151.18 (Ar).

345TMP-m. Pale yellow cubic crystals. Purity: 99.90%. ^{1}H NMR (200 MHz, $CDCl_3$, 298K): δ 2.09 (2), 2.21 (Ar−CH_3), 2.59 (N−CH_3), 3.82 (Ar−CH_2−N), 4.74 (N−CH_2−O), 6.58 (Ar−H). ^{13}C NMR (200 MHz, $CDCl_3$, 298K): δ 14.36 (Ar−C), 14.60 (Ar−C), 20.35 (Ar−C), 30.70 (N−C), 50.45 (Ar−C−N), 82.24 (O−C−N), 114.64 (Ar), 116.05 (Ar), 126.31 (Ar), 133.81 (Ar), 134.57 (Ar), 150.93 (Ar).

Polymer Synthesis. A typical polymerization procedure is described below: A 100 mL round-bottomed flask was flame-dried under vacuum and filled with argon. A magnetic stir bar was added, and the flask fitted with a rubber septum. The monomer solution in chloroform (2 M) was introduced by syringe and allowed to thermally equilibrate at the reaction temperature (ca. −60 °C), then the catalyst solution, phosphorus pentachloride (PCl_5) in chloroform (40 mM), was injected, and the polymerization was allowed to proceed for 72 h. After the desired reaction time, the polymerization was terminated by methanol. The polymer was then precipitated out by 300 mL of ethyl ether/hexane. The precipitated polybenzoxazine was isolated by filtration, washed with tetrahydrofuran, and dried at room temperature under vacuum.

Instrumentation. Gas chromatography/mass spectroscopy (GC/MS) analysis was performed on a Hewlett-Packard 6890 gas chromatograph coupled with a 5973 mass selective detector. A nonbonded capillary column coated with 5% phenyl−methyl siloxane was used. The MS operates at an ionization energy of 70 eV. Helium carrier gas was used at a flow rate of 1 mL/min. The injection port of the GC was held at 250 °C while the GC column was heated from 70 to 280 °C at a heating rate of 8 °C/min. The 30 largest chromatogram peaks in each sample were integrated. ^{1}H nuclear magnetic resonance (NMR) spectra were collected on a 200 MHz Varian XL-200 NMR spectrometer. The ^{13}C NMR spectra were recorded on the same spectrometer with proton decoupling. Both deuterated chloroform and dimethyl sulfoxide (DMSO) were used as solvent depending on the solubility of the examined materials. Fourier transform infrared (FT-IR) spectra were taken on a Biorad FTS-60A Fourier transform infrared spectrometer which was equipped with a liquid nitrogen-cooled, linearized mercury−cadmium−telluride (MCT) detector. Spectra were recorded at a resolution of 4 cm^{-1} with 256 coadded scans. The samples were cast as thin films on KBr plates or finely ground with KBr powder and pressed into pellets. Elemental analysis was performed by Galbraith Laboratories. Static light scattering (SLS) experiments were performed on a Brookhaven Instrument Corp. spectrometer with a Spectraphysics 15 mW He/Ne laser (λ = 632.8 nm) at 25 °C. All measurements were made from 20 to 120° scattering angles. Size exclusion chromatography (SEC) was performed on a Waters Maxima 820 workstation equipped with three Styrogel columns with pore sizes of 50, 10^2, and 10^3 nm, respectively, and with a 256 nm fixed wavelength ultraviolet (UV) detector and a refractive index (RI) detector. Chloroform was used as the solvent. A size 1 Ubbelohde viscometer from Cannon Instrument Co. was utilized to obtain the viscosity data of the four as-synthesized polymers. DMSO was used as the solvent. The experiments were carried out at 25 °C. Differential scanning calorimetry (DSC) measurements were performed on a TA Instruments 2910 high-pressure DSC with a heating rate of 10 °C/min under 2.76 MPa pressure generated by dry nitrogen. Thermogravimetric analysis (TGA) was performed on a TA Instruments 2950 model high-res. TGA at a heating rate of 10 °C/min under a 90 mL/min nitrogen flow. Wide-angle X-ray diffraction (WAXD) experiments were performed on a Philips XRG 3100 X-ray generator, using Ni-filtered Cu Kα X-ray radiation. For the molecular modeling of benzoxazine monomer, the SYBYL software package was used. The MAXIMIN2 subroutine of the SYBYL software package was used to determine the energy-minimized structure. Atomic coordinates, obtained from the crystallographic study reported by Dunkers and Ishida,[22] were used as the starting structure prior to the energy minimization and charge calculation.

Results and Discussion

Proposed Mechanisms. A single-crystal X-ray crystallographic study[22] shows that the preferential confor-

Scheme 2. Polymerization Mechanism A

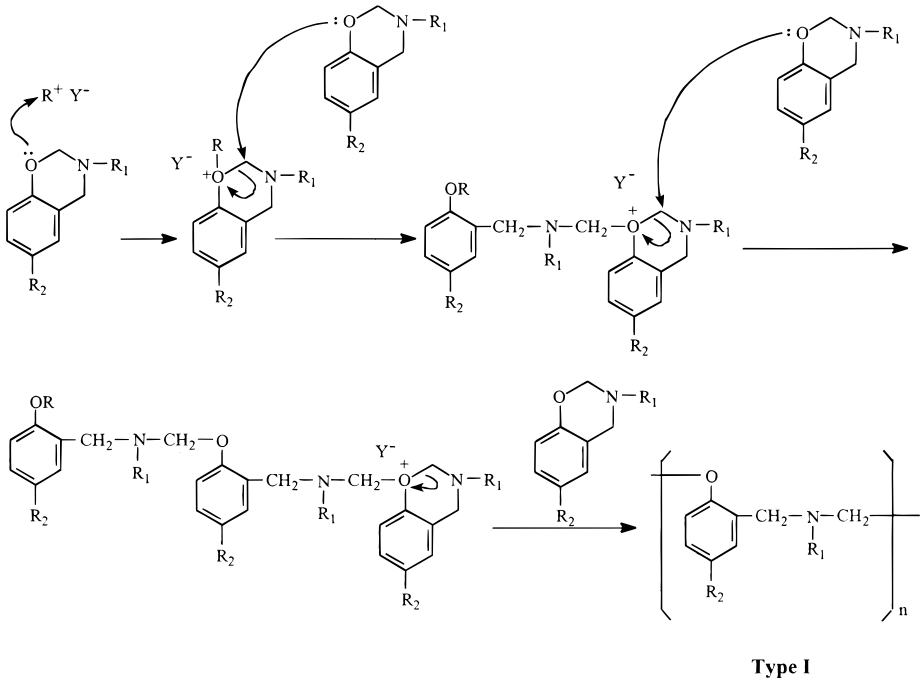

Type I

mation of a mono-oxazine ring containing benzoxazine is a distorted semichair structure, with the nitrogen and the carbon between the oxygen and nitrogen on the oxazine ring sitting, respectively, above and below the benzene ring plane. The resulting ring strain from this molecular conformation makes it possible for this type of six-membered ring containing molecule to undergo ring-opening polymerization under certain conditions. In addition, from the chemistry point of view, both the oxygen and the nitrogen on the oxazine ring can be potential cationic polymerization initiation sites due to their high basicity by Lewis definition. The electron charge calculation after energy minimization predicts, however, that oxygen might be the preferred polymerization site over nitrogen due to its high negative charge distribution (O, −0.311; N, −0.270). In light of this knowledge, we propose that the oxygen on the oxazine ring will act as the initiation site, upon attack of a cationic initiator, to form a cyclic tertiary oxonium ion. The polymerization will then proceed by insertion of the monomers through the reaction of the oxygen on the oxazine ring, thereby leading to a Mannich base phenoxy-type (Type I) polybenzoxazine structure. This mechanism is illustrated as mechanism A in Scheme 2. Also, an alternative polymerization route which is similar to mechanism A but having N as the initiation and propagation sites can be proposed (Scheme 3). This mechanism could also lead to the formation of a Mannich base phenoxy-type (Type I) polybenzoxazine structure. Furthermore, in a benzoxazine molecule, other than the electron-rich nitrogen and oxygen, the unobstructed ortho position of the benzene ring with respect to the phenoxy OR group is well-proven to possess high reactivity toward thermal polymerization of benzoxazines with or without catalysts.[17,22] Therefore, it is logical to assume that upon initiation by a cationic initiator, the propagation can also proceed by insertion of the monomers through the reaction of the unobstructed benzene ortho position, producing a Mannich base phenolic-type (Type II) polymer. This proposed mechanism is illustrated as mechanism B in Scheme 4. Moreover, in this latter case, the monomers propagate via reasonably stable carbocations, i.e., oxonium cations stabilized by intramolecular hydrogen bonding (as shown in Scheme 4), which could lead to high-molecular-weight polymer formation.[23] In the present work, we expect that the polymerization of the selected four mono-oxazine ring containing benzoxazine monomers will follow the above-proposed mechanisms.

Structural Characterization. *(a) NMR Analysis.* The ^{1}H NMR spectra of the four as-synthesized polymers derived from 24DMP-m (Figure 1A), 235TMP-m (Figure 1B), 345TMP-m (Figure 1C), and *p*C-m (Figure 1D) are presented in Figure 1. As stated in the above-proposed mechanisms, aside from the different substitutions on the benzene ring, the difference between the Type I polymer structure and that of the Type II can be distinguished by the chemical environment of the two methylene groups between adjacent aromatic rings. In the Type I polymer structure, two kinds of methylene group exist. In contrast, only one kind of methylene group exists in the Type II polymer repeating unit. With this understanding, analysis of the ^{1}H NMR spectra will focus on the 3−6 ppm chemical shift range, which is usually the proton NMR shift range of aliphatic methylene groups next to aromatic ring or heteroatoms.[24]

Inspection of the ^{1}H NMR spectrum of poly(24DMP-m), as shown in Figure 1A, reveals two resonances at respective chemical shifts of 4.3 and 5.1 ppm with equal integrated intensities. A similar feature has also been observed for poly(235TMP-m) (Figure 1B), which shows two resonances at 4.2 and 5.0 ppm. This implies that two different methylene groups exist in the repeating unit of both poly(24DMP-m) and poly(235TMP-m), which can be tentatively assigned as the Type I polymer structure formed via mechanism A. Examination of the ^{1}H NMR spectrum of poly(345TMP-m) (Figure 1C), whose monomer possesses an unobstructed ortho position on the benzene ring, reveals that, aside from the same feature observed in the spectra of poly(24DMP-m) and poly(235TMP-m), i.e., two major methylene proton resonances at 4.3 and 5.0 ppm, another interest-

Scheme 3. Alternative of Polymerization Mechanism A

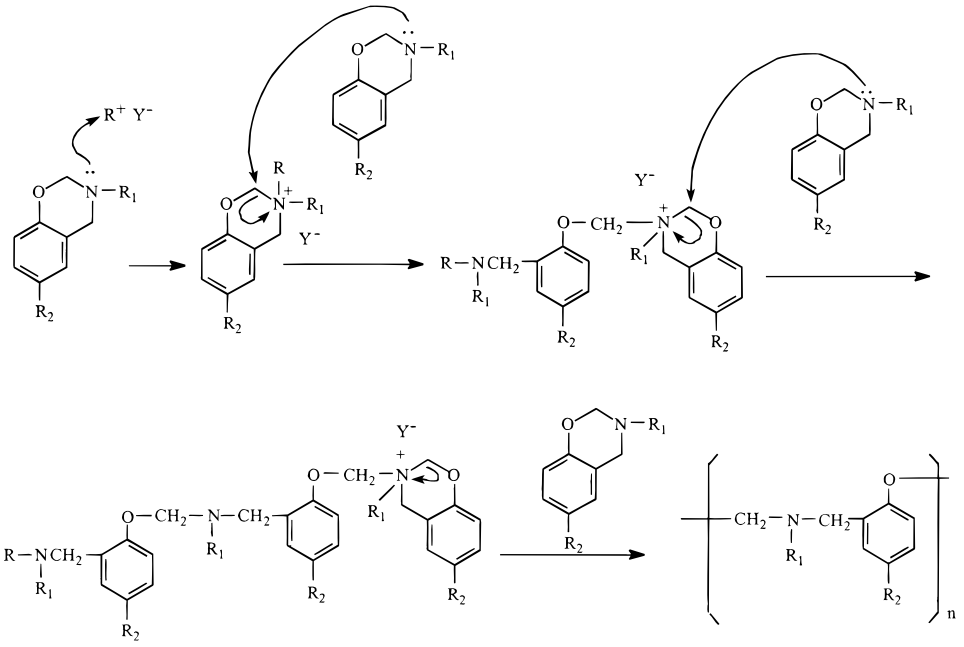

Type I

Scheme 4. Polymerization Mechanism B

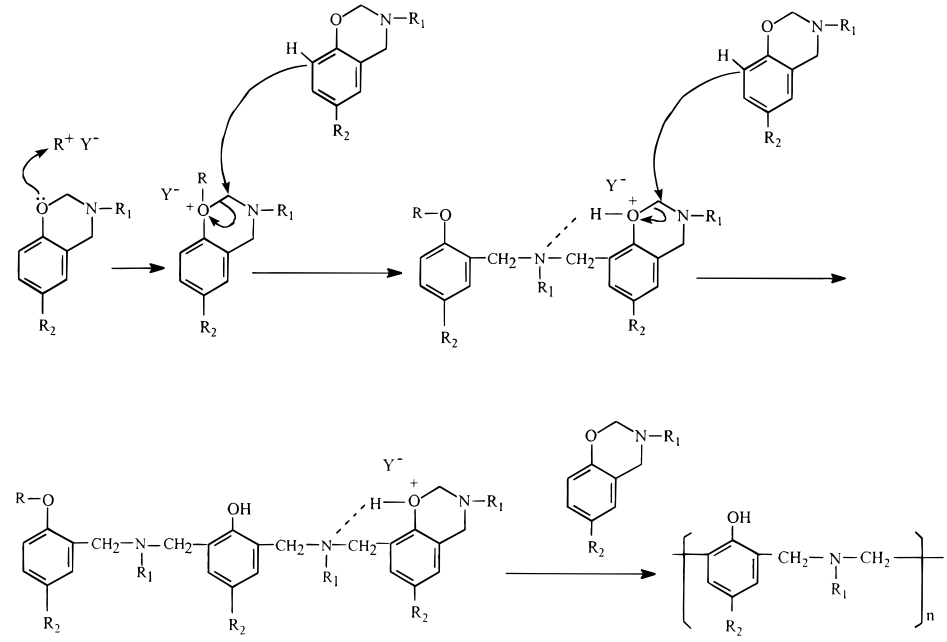

Type II

ing resonance is also present at a chemical shift of 3.9 ppm. The resonance usually appearing in this vicinity in polybenzoxazine chemistry has been assigned to the proton of the symmetric Mannich base bridge ($-CH_2-N-CH_2-$) formed via mechanisms[16,17] similar to mechanism B. This evidence further implies that other than the major polymerization via mechanism A, the unobstructed ortho position on the benzene ring also partially participates in the polymerization of 345TMP-m via mechanism B, rendering a small portion of the phenolic-type (Type II**)** polymer structure. Quantitative comparison of the methylene protons assigned to the two different polymer structures reveals a 9:1 ratio for the resonances of the Mannich base phenoxy-type (Type I) and the Mannich base phenolic-type (Type II) polybenzoxazines.

Of particularly interest is the ^{1}H NMR spectrum of poly(*p*C-m). As shown in Figure 1D in the examined aliphatic methylene proton resonance region, only one distinguishable resonance centered at 4.0 ppm is observed, indicating a critical structural difference between poly(*p*C-m) and poly(24DMP-m) or poly(235TMP-m). Consequently, instead of having methylene groups with different chemical environments in the molecule, both of the methylene groups in the poly(*p*C-m) repeating unit are chemically equivalent. Furthermore, a

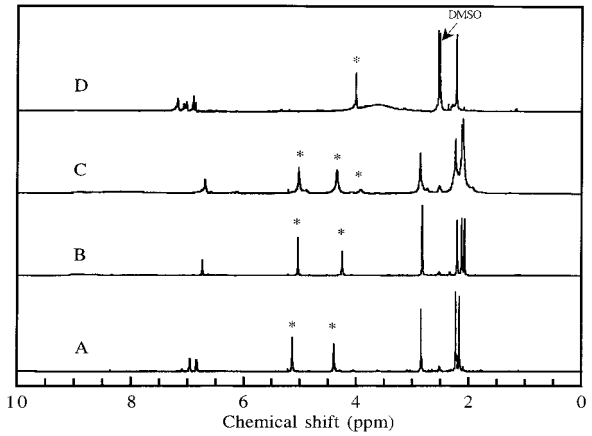

Figure 1. ^{1}H NMR spectra of as-synthesized (A) poly(24DMP-m), (B) poly(235TMP-m), (C) poly(345TMP-m), and (D) poly(*p*C-m) in DMSO-d_6 at room temperature.

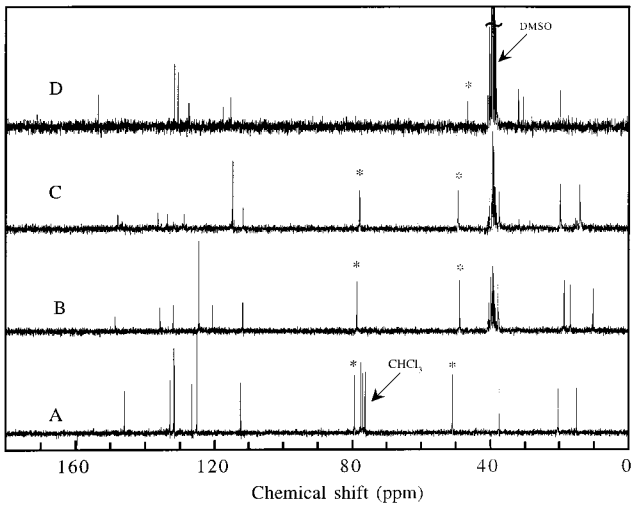

Figure 2. ^{13}C NMR spectra of as-synthesized (A) poly(24DMP-m) in chloroform-d_1, (B) poly(235TMP-m), (C) poly(345TMP-m), and (D) poly(*p*C-m) in DMSO-d_6 at room temperature.

broad hump centered at 3.6 ppm is also observed in this spectrum, which is cited as evidence of the existence of hydroxyl groups in this molecule. Together, these two features of poly(*p*C-m) are consistent with the Type II phenolic polybenzoxazine structure formed via mechanism B.

In addition to ^{1}H NMR analysis, ^{13}C NMR has also been utilized to determine the structure of these four polymers. Shown in Figure 2 are the ^{13}C NMR spectra of poly(24DMP-m) (Figure 2A), poly(235TMP-m) (Figure 2B), poly(345TMP-m) (Figure 2C), and poly(*p*C-m) (Figure 2D). In each instance, the resonances below 40 ppm are assigned to the methyl carbons in the repeating unit, and the number of resonances depends on the different monomer structures used. The resonances between 40 and 90 ppm are assigned to the aliphatic methylene carbons, and the resonances between 110 and 160 ppm are assigned to the aromatic carbons in the polymer structure. As mentioned before, to differentiate the polymer structures, an examination of the methylene carbon resonance region becomes particularly helpful. As can be seen in Figures 2A−C, each spectrum contains two major resonances in this region, with the resonance around 80 ppm being assigned to the methylene carbon in the $-N-CH_2-O-$ structure and the resonance around 50 ppm to the $-N-CH_2-Ar-$ structure.[24] This

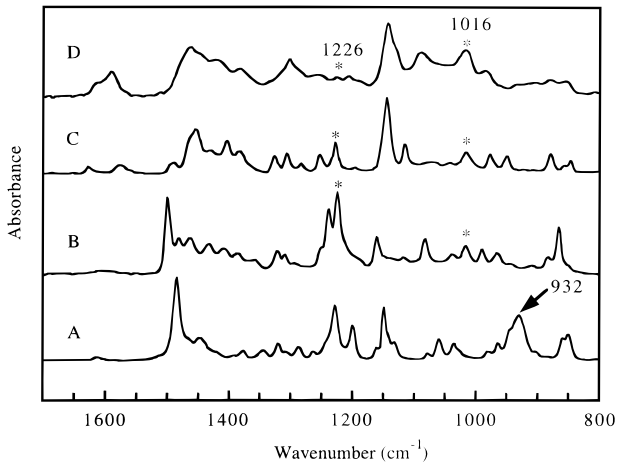

Figure 3. FT-IR spectra of (A) 24DMP-m monomer and as-synthesized (B) poly(24DMP-m), (C) poly(235TMP-m), and (D) poly(345TMP-m) in the 1700−800 cm^{-1} region.

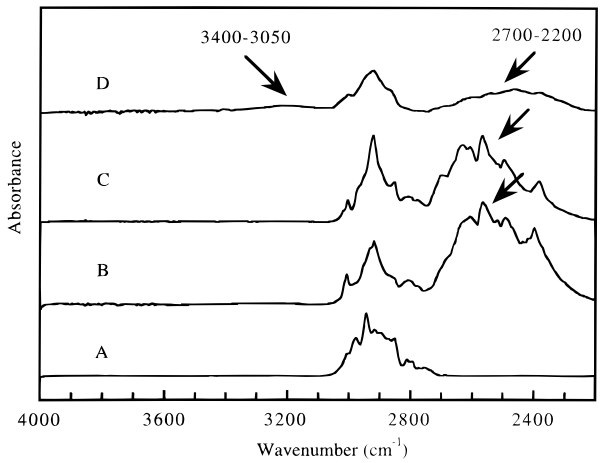

Figure 4. FT-IR spectra of (A) 24DMP-m monomer and as-synthesized (B) poly(24DMP-m), (C) poly(235TMP-m), and (D) poly(345TMP-m) in the 4000−2200 cm^{-1} region.

observation supports the Mannich base phenoxy (Type I) structure discussed in the ^{1}H NMR analysis of poly(24DMP-m), poly(235TMP-m) and poly(345TMP-m).

Like ^{1}H NMR, the ^{13}C NMR spectrum of poly(*p*C-m) again distinguishes itself from the other three polymers by only showing one resonance around 47 ppm in the methylene carbon resonance region. The absence of the resonance around 80 ppm indicates the lack of the $-N-CH_2-O-$ moiety in the polymer structure, which is consistent with the Type II phenolic structure proposed in the previous ^{1}H NMR analysis. The two resonances around 31 ppm can both be assigned to the methyl carbon connected to the nitrogen in the polymer structure. These resonances may come from the partial alkylammonium chloride salt formation of the nitrogens, which will be discussed further in the following FT-IR and elemental analyses.

(b) FT-IR Analysis. Figures 3−6 present the FT-IR spectra of the four as-synthesized polymers. Among them, Figure 3 shows the 1700−800 cm^{-1} FT-IR region of poly(24DMP-m), poly(235TMP-m), and poly(345TMP-m). The FT-IR feature of poly(*p*C-m) in this region is presented in Figure 5. Figure 4 shows the 4000−2200 cm^{-1} FT-IR region of poly(24DMP-m), poly(235TMP-m), and poly(345TMP-m). Figure 6 presents poly(*p*C-m) in the 4000−2200 cm^{-1} region. Four structurally related features can be rationalized from these figures. The first

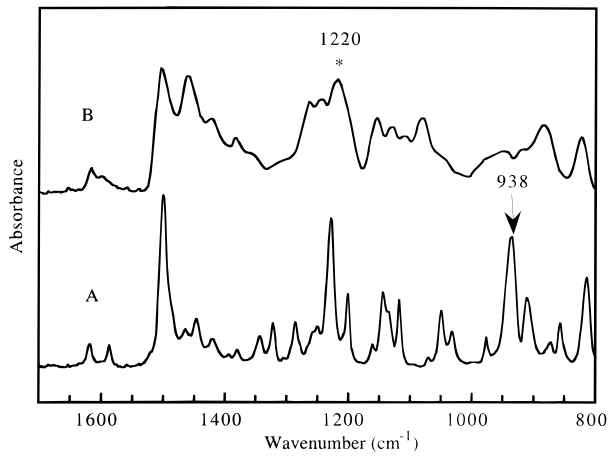

Figure 5. FT-IR spectra of (A) *p*C-m monomer and (B) as-synthesized poly(*p*C-m) in the 1700−800 cm^{-1} region.

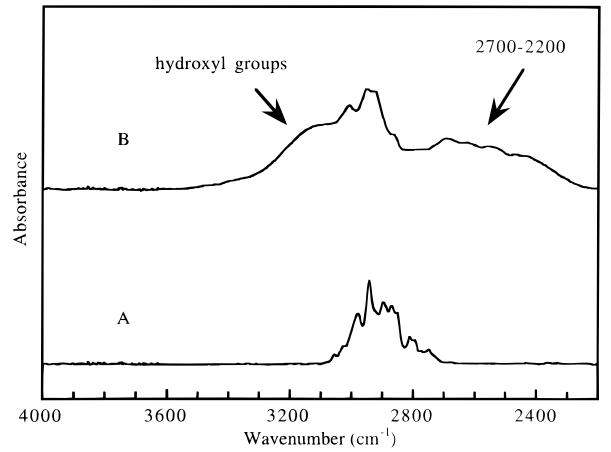

Figure 6. FT-IR spectra of (A) *p*C-m monomer and (B) as-synthesized poly(*p*C-m) in the 4000−2200 cm^{-1} region.

is the absorption band around 930 cm^{-1} (indicated by an arrow) in the monomer spectra, irrespective of the monomer structure. This band could be viewed as a characteristic of the oxazine ring, which has been attributed to either a −C−O−C− cyclic acetal vibrational mode[25] or a C−H out-of-plane deformation (mode 10a).[21] As expected, this band disappears in each of the polymer spectra, demonstrating the successful opening of the oxazine rings upon cationic polymerization.

The second important feature is the pair of correlated bands around 1226 and 1016 cm^{-1} in the spectra of poly(24DMP-m), poly(235TMP-m), and poly(345TMP-m) (indicated by an asterisk). Usually, an alkoxyl on an aromatic ring gives rise to two correlatable bands at 1310−1210 cm^{-1} and 1050−1010 cm^{-1}.[26,27] The band near 1226 cm^{-1} corresponds to an aromatic carbon−oxygen stretching frequency as in phenols, and the band near 1016 cm^{-1} can be viewed as the highest aliphatic carbon−oxygen stretching frequency as in primary alcohols. Both of these bands are observed for poly(24DMP-m), poly(235TMP-m), and poly(345TMP-m) in Figure 3, indicating the existence of −C−O−Ar moieties in these polymer structures, which correlates with the Mannich base phenoxy-type structure (Type I) of these polymers as determined by NMR analysis. For poly(*p*C-m), however, no correlatable band can be detected in the region of 1050−1010 cm^{-1}, as shown in Figure 5, indicating the lack of the primary alcohol like aliphatic C−O stretching in this polymer. Instead, only the aromatic C−O stretching frequency like that of phenols exists. This observation is in good agreement with the phenolic-type (Type II) structure of this polymer.

Scheme 5. Salt Structure of (A) Type I and (B) Type II Polymer Repeating Unit

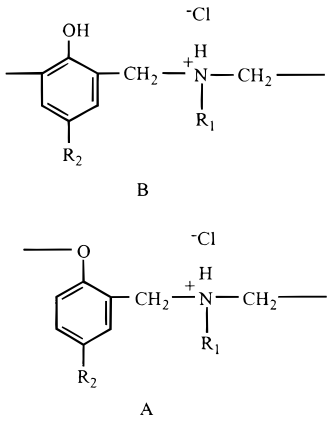

The third distinguishing feature of these figures is the 3700−3100 cm^{-1} OH stretching vibrational region. As can be seen in Figure 4, there is no absorption band in the 3700−3100 cm^{-1} OH stretching region in either the spectra of poly(24DMP-m) (Figure 4B) or poly(235TMP-m) (Figure 4C), indicating the lack of OH groups in these two polymer structures. For poly(345TMP-m), however, a weak, yet broad band appears at 3400−3050 cm^{-1} (Figure 4D), indicating the existence of a small amount of hydrogen-bonded OH groups in the polymer structure. As for poly(*p*C-m) (Figure 6B), a broad and intense band appears at approximately 3500 cm^{-1} until it becomes overlapped with the C−H stretching bands around 3000 cm^{-1}, indicating the existence of a high concentration of hydrogen-bonded hydroxyl groups. This third feature of these polymer FT-IR spectra is also in excellent agreement with the polymerization mechanisms and polymer structures based on the previous NMR analysis, i.e., the Mannich base phenoxy-type structure (Type I) for poly(24DMP-m) and poly(235TMP-m), the Mannich base phenolic-type structure (Type II) for poly(*p*C-m), and the mixed structure for poly(345TMP-m) with the phenoxy type as the major component.

And finally, there is a fourth feature which can be seen in all of the four polymer FT-IR spectra as shown in Figures 4B−D and 6B (the existence of multiple bands in the region of 2700−2200 cm^{-1}), which is a characteristic feature of a $R_3N^+H\ Cl^-$ structure.[28] In light of this knowledge, we propose an alkylammonium chloride salt formation as shown in Scheme 5. As mentioned previously, methanol was added into the system to terminate the polymerization and thus may generate hydrochloric acid which can further react with the N on the polymer chain to form a $R_3N^+H\ Cl^-$ salt structure. Further elemental analysis supports this salt formation hypothesis. As will be mentioned below, poly(*p*C-m) obtained from this cationic polymerization process is a water-soluble material. This kind of hydrophilic property has never been reported for thermally polymerized benzoxazine polymers. The well-accepted polybenzoxazine structure via thermal polymerization can also be thought of as the Type II polymer structure which can be generated through mechanisms similar to mechanism B. Despite the existence of a high concentration of hydroxyl groups, polymers with this structure are hydrophobic due to the extensive inter-

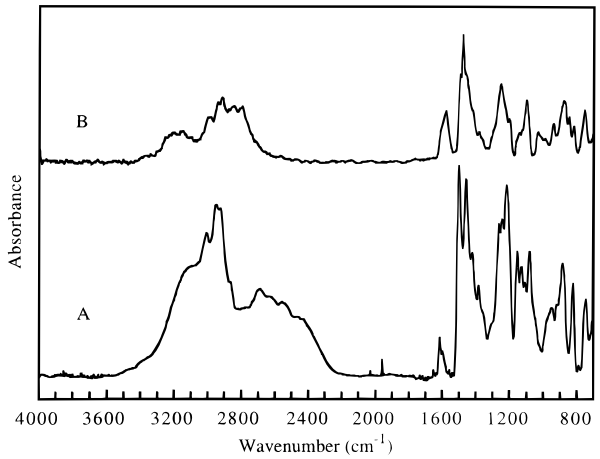

Figure 7. Comparison of the FT-IR spectra of (A) as-synthesized poly(*p*C-m) and (B) poly(*p*C-m) after treated with 2 N aqueous NaOH solution.

and intramolecular hydrogen bonding of the hydroxyl groups.[30,31] However, owing to the above-proposed salt formation on the nitrogen atoms, the intramolecular hydrogen bonding between the hydroxyl group and the nitrogen is inhibited in the as-synthesized poly(*p*C-m) under investigation. The hydroxyl groups, thus, are possibly loosely intermolecularly hydrogen-bonded, which may easily be interrupted by water molecules, resulting in the unusual hydrophilic property of this polymer. In addition, the alkylammonium chloride salt moieties on the polymer chain are also very likely to interact with the water molecules, which further contributes to the hydrophilic nature of poly(*p*C-m). To ascertain this hypothesis, the as-synthesized water-soluble poly(*p*C-m) was further treated with 2 N aqueous sodium hydroxide (NaOH) solution. We expect that, upon reaction with NaOH, the salt structure as shown in Scheme 5B would change back to the Type II polymer structure, and that the resulting product should no longer be soluble in water, and indeed, the NaOH-treated polymer did not dissolve in water. Furthermore, as shown in Figure 7, the multiple bands at 2700−2200 cm^{-1} were no longer observed (Figure 7B), indicating the disappearance of the $R_3N^+H\ Cl^-$ structure upon the treatment by NaOH.

To further verify the proposed polymer structure, elemental analysis was performed on poly(*p*C-m). The experimental result (C, 59.37 ± 0.25%; H, 7.06 ± 0.16%; N, 6.35 ± 0.04%; Cl, 14.92 ± 0.34%) is in reasonable agreement with the calculated value (C, 60.15%; H, 7.02%; N, 7.01%; Cl, 17.79%) based on the repeating salt structure in Scheme 5B. A large amount of chlorine was found in the as-synthesized poly(*p*C-m), which supports the hypothesis of the salt formation. It is interesting to note the significant discrepancy between the calculated value of chlorine and the one determined experimentally. The lower amount of chlorine in the product may indicate incomplete salt formation on the nitrogens in the polymer chain, assuming that salt formation may take place in each chemical repeat unit.

The molecular weight of the phenoxy-type (Type I) polymers was measured by SEC with chloroform as eluent. In the case of poly(235TMP-m), it was first dissolved in DMSO and then diluted with chloroform. The molecular weights of poly(24DMP-m), poly(235TMP-m), and poly(345TMP-m), with polystyrene as standard, are 1500, 6500, and 3950, respectively. Static light

Table 1. Summary of the Characterization Data of the Four Polybenzoxazines

sample	repeating unit*	$[\eta]_{DMSO}$ at 25°C ($cm^3\ g^{-1}$)	molecular weight
poly(24DMP-m)	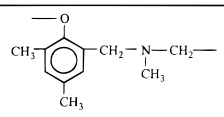	1.7	1500[a]
poly(235TMP-m)	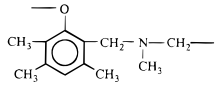	5.2	6500[a]
poly(345TMP-m)	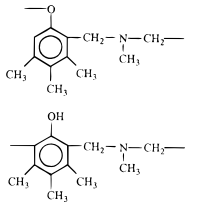	3.5	3950[a]
poly(*p*C-m)	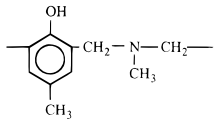	12	55,000[b]

* Salt structure is not included. [a] SEC. [b] Light scattering.

scattering was utilized to measure the molecular weight of poly(*p*C-m), which, as estimated by NMR end group analysis, has a high number-average molecular weight. The weight-average molecular weight of poly(*p*C-m) obtained from the Zimm plot is in the vicinity of 55 000. Intrinsic viscosities of these polymers in DMSO at 25 °C are 1.7 cm^3 g^{-1} for poly(24DMP-m), 5.2 cm^3 g^{-1} for poly(235TMP-m), 3.5 cm^3 g^{-1} for poly(345TMP-m), and 12 cm^3 g^{-1} for poly(*p*C-m). A summary of all of the characterization data for these four polymers is tabulated in Table 1.

Polymer Properties. Both hydrophobic and hydrophilic thermoplastic polybenzoxazines have been generated depending on the different monomers used. A summary of the solubility of the four as-synthesized polymers is given in Table 2.

Thermal characterization of these polymers was accomplished by DSC and TGA. Figure 8 depicts the first DSC heating curves of the as-synthesized polybenzoxazines from 24DMP-m, 235TMP-m, 345TMP-m, and *p*C-m. A melting transition as well as glass transition (T_g) are detected for poly(24DMP-m), poly(235TMP-m), and poly(345TMP-m). Their DSC thermograms present well-defined melting peaks at 183, 187, and 196 °C, respectively, indicating a significant amount of crystallinity in each. The corresponding T_g's of these three polymers are 51, 77, and 89 °C, respectively. The second DSC heating curves were not attempted because of the degradation of these polymers in the melt state. Poly(*p*C-m) shows only a broad glass transition around 115 °C without any significant melting behavior being detected in the tested temperature range, indicating a lack of crystallinity in the as-synthesized poly(*p*C-m). The second DSC heating curve of this polymer shows the same feature as that in Figure 8A. The results of the TGA experiments of these polymers are shown in Figure 9. It can be seen that, except for the polymer derived from 24DMP-m, which has a relatively low

Table 2. Solubility of the Four As-Synthesized Polymers[a]

polymers from	solvent[b]							
	$CHCl_3$	THF	acetone	DMSO	DMF	methanol	toluene	H_2O
24DMP-m	+	−	+	+	+	−	−	−
235TMP-m	−	−	−	+	+	−	−	−
345TMP-m	+	−	−	+	+	−	−	+−
*p*C-m	−	−	−	+	+	−	−	+

[a] Solubility: +, soluble at room temperature; +−, partially soluble; and -, insoluble. [b] THF, tetrahydrofuran; DMSO, dimethyl sulfoxide; DMF, *N*,*N*-dimethylformamide.

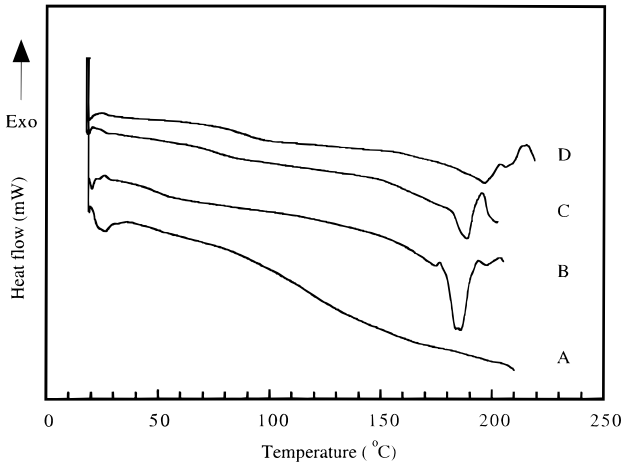

Figure 8. DSC thermograms (1st heating curves) of as-synthesized (A) poly(*p*C-m), (B) poly(24DMP-m), (C) poly(235TMP-m), and (D) poly(345TMP-m).

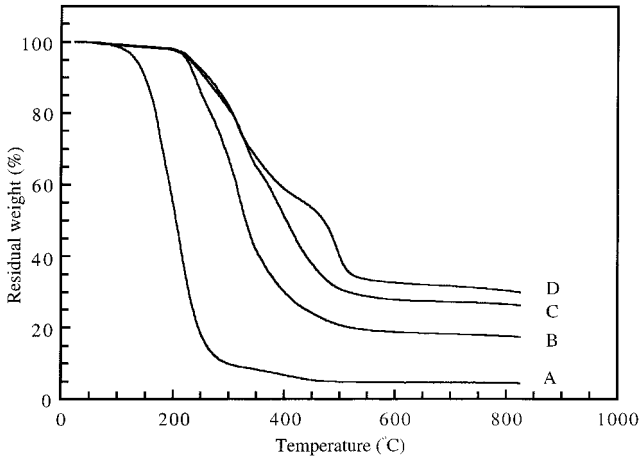

Figure 9. TGA thermograms of the as-synthesized (A) poly(24DMP-m), (B) poly(235TMP-m), (C) poly(345TMP-m), and (D) poly(*p*C-m).

molecular weight, the other three polymers remain fairly stable up to 220 °C, with the char yields at 800 °C under nitrogen of 17.7%, 26.6%, and 30.4%, corresponding to those of the polymers obtained from 235TMP-m, 345TMP-m, and *p*C-m, respectively. Furthermore, the TGA degradation pattern of poly(*p*C-m) appears to be significantly different from those of poly(24DMP-m) and poly(235TMP-m), which may be attributed to their different structures.

The most important aspect of this work is the discovery that by using a proper initiator and mono-oxazine ring containing benzoxazine monomers, both linear semicrystalline and amorphous polybenzoxazines can be synthesized. All past work on polybenzoxazines were based on their thermoset nature except for a few reports of oligomer synthesis. Here, we have synthesized and

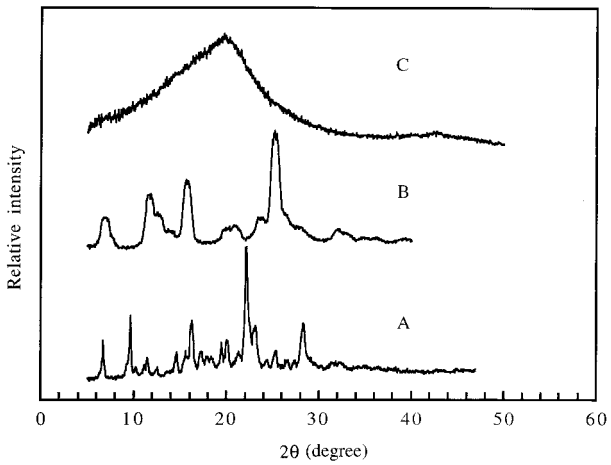

Figure 10. X-ray powder diffraction patterns of as-synthesized (A) poly(24DMP-m), (B) poly(235TMP-m), and (C) poly(*p*C-m).

verified for the first time thermoplastic polybenzoxazines with significant molecular weights. To further investigate the semicrystalline or amorphous nature of these polybenzoxazines, wide-angle X-ray powder diffraction was also utilized. Figure 10 shows the WAXD results of the three polybenzoxazines. It seems that both poly(24DMP-m) and poly(235TMP-m) show diffraction patterns which are typical for semicrystalline materials. For poly(24DMP-m), the major diffraction peaks appear at $2\theta = 6.7°$, 9.6°, 16.3°, 19.5°, 22.1°, and 28.3°, corresponding to 1.32, 0.92, 0.54, 0.46, 0.40, and 0.32 nm *d* spacings. For poly(235TMP-m), the major diffraction peaks appear at $2\theta = 6.8°$, 11.8°, 15.6°, 20.8°, 23.9°, 25.2°, and 32.2°, corresponding to 1.30, 0.75, 0.57, 0.42, 0.37, 0.35, and 0.28 nm *d* spacings. The crystallinity estimated from the WAXD pattern is 68% for poly(24DMP-m) and 78% for poly(235TMP-m). X-ray diffraction analysis of poly(*p*C-m) revealed a large amorphous hump between approximately $2\theta = 10$ and 30° and little evidence of crystallographic reflections. This result is consistent with the lack of observable melting transition observed from the DSC analysis.

Conclusions

New thermoplastic polybenzoxazines were synthesized by cationic ring-opening polymerization of substituted 3-methyl-3,4-dihydro-2*H*-1,3-benzoxazines with PCl_5 as an initiator. Depending on the different substitution positions of the monomers, two different polymerization mechanisms competed during the polymerization process, giving rise to both phenoxy-type and phenolic-type polymers. Both semicrystalline and amorphous thermoplastic polybenzoxazines were obtained.

Acknowledgment. The authors gratefully acknowledge the financial support of the NSF Center for Molecular and Microstructure of Composites (CMMC),

which is jointly established with the State of Ohio and EPIC, representing the industrial members.

References and Notes

(1) Holly, F. W.; Cope, A. C. *J. Am. Chem. Soc.* **1944**, *66*, 1875.
(2) Burke, W. J. *J. Am. Chem. Soc.* **1949**, *71*, 609.
(3) Burke, W. J.; Weatherbee, C. *J. Am. Chem. Soc.* **1950**, *72*, 4691.
(4) Burke, W. J.; Stephens, C. W. *J. Am. Chem. Soc.* **1952**, *74*, 1518.
(5) Burke, W. J.; Murdoch, K. C.; Ec, G. *J. Am. Chem. Soc.* **1954**, *76*, 1677.
(6) Burke, W. J.; Glennie, E. L. M.; Weatherbee, C. *J. Org. Chem.* **1964**, *24*, 909.
(7) Moloney, G. P.; Craik, D. J.; Iskander, M. N. *J. Pharm. Sci.* **1992**, *81*, 692.
(8) Gammill, R. B. *J. Org. Chem.* **1981**, *46*, 3340.
(9) Chylinska, J. B.; Urbanski, T. *Br. J. Pharmacol.* **1971**, *43*, 649.
(10) Ning, X.; Ishida, H. *J. Polym. Sci., Polym. Chem.* **1994**, *32*, 1121.
(11) Ishida, H.; Allen, D. J. *J. Polym. Sci., Phys. Ed.* **1996**, *34*, 1019.
(12) Shen, S. B.; Ishida, H. *Polym. Composites* **1996**, *17*, 711.
(13) Burke, W. J.; Bishop, J. L.; Glennie, E. L. M.; Bauer, W. N., Jr. *J. Org. Chem.* **1965**, *30*, 3423.
(14) Riess, G.; Schwob, J. M.; Guth, G.; Roche, M.; Lande, B. In *Advances in Polymer Synthesis*; Culbertson, B. M., McGrath, J. E., Eds., Plenum: New York, 1986.
(15) Ishida, H.; Rodriguez, Y. *J. Appl. Polym. Sci.* **1995**, *58*, 1751.
(16) Dunkers, J.; Ishida, H. *J. Polym. Sci., Polym. Chem. Ed.* **1999**, *37*, 1913.
(17) Cid, J. A.; Wang, Y. X.; Ishida, H. *Polym. Polym. Composites* **1999**, *7*, 409.
(18) Gu, Y.; Lu, Z.; Xie, M.; Miao, S.; Du, R.; Cai, X. *Gong Cheng Su Liao Ying Yong (Chinese)* **1996**, 3.
(19) Pei, D.; Gu, Y.; Li, Z.; Cai, X. *Polym. Mater. Sci. Eng. (Chinese)* **1997**, *13*, 43.
(20) Wang, Y. X.; Ishida, H. *Polymer* **1999**, *40*, 4563.
(21) Dunkers, J.; Ishida, H. *Spectrochim. Acta* **1995**, *51A*, 855.
(22) Dunkers, J.; Zarate, E. A.; Ishida, H. *Polymer*, submitted for publication.
(23) Odian, G. *Principle of Polymerization*, 3rd ed.; John Wiley & Sons: 1991; Chapter 5.
(24) Lambert, J. B.; Shurvell, H. F.; Lightner, D. A.; Cooks, R. G. *Organic Structural Spectroscopy*; Prentice-Hall: 1998.
(25) Eckstein, Z.; Gluzinski, P.; Hofman, W.; Urbanski, T. *J. Chem. Soc.* **1961**, 489.
(26) Katritzky, A. R.; Coats, N. A. *J. Chem. Soc.* **(**London**)1959**, 2062.
(27) Sax, K. J.; Saari, W. S.; Mahoney, C. L.; Gordon, J. M. *J. Org. Chem.* **1960**, *25*, 1590.
(28) Colthup, N. B.; Daly, L. H.; Wiberley, S. E. *Introduction to Infrared and Raman Spectroscopy*, 3rd ed.; Academic Press: 1990; Chapter 10.
(29) Morrison, R. T. *Organic Chemistry*, 6th ed.; Prentice Hall Inc.: New Jersey, 1992; Chapters 22 & 23.
(30) Schenell, I.; Brown, S. P.; Low, H. Y.; Ishida, H.; Spiess, H. W. *J. Am. Chem. Soc.* **1998**, *120*, 11784.
(31) Dunkers, J.; Zarate, E. A.; Ishida, H. *J. Phys. Chem.* **1996**, *100*, 13514.

MA9909096